The role of nucleation in vitrification of supercooled liquids



2010 J. Phys.: Condens. Matter 22 155108

(http://iopscience.iop.org/0953-8984/22/15/155108)

J. Phys.: Condens. Matter **22** (2010) 155108 (8pp) doi:10.1088/0953-8984/22/15/155108

# The role of nucleation in vitrification of supercooled liquids

**J Baran**[1], **N A Davydova**[2,3] **and M Drozd**[1]

[1] Institute of Low Temperature and Structure Research, PAS, 50-950, Wroclaw, Poland
[2] Institute of Physics, NANU, 46, pr. Nauki, 03028, Kiev, Ukraine

E-mail: davydova@iop.kiev.ua

Received 5 November 2009, in final form 22 February 2010
Published 23 March 2010
Online at stacks.iop.org/JPhysCM/22/155108

**Abstract**
Low-frequency Raman and differential scanning calorimetry (DSC) investigations were carried out during a structural transformation of supercooled liquid salol (phenyl salicylate) in a wide temperature range. DSC experiments indicate that in the supercooled liquid salol at temperature ∼40 K above the glass transition temperature metastable nuclei start to form. During subsequent cooling the nuclei become an important element of the glass structure, and thereby are considered as a measure of the intermediate range order in this glass. It was shown that the crystalline structure of the metastable nuclei differ from that of the stable nuclei. Low-frequency Raman spectra of the glassy salol show a broad band in the spectral range from 14.5 to 17.2 $cm^{-1}$; the so called 'Boson peak', which can be interpreted in terms of its relationship to the formation of structured clusters, with typical sizes in the nanometer range (critical radii).

(Some figures in this article are in colour only in the electronic version)

## 1. Introduction

A variety of glass-forming liquids show different dynamics above and below a crossover temperature $T_c \approx 1.2T_g$ ($T_g$ is the glass transition temperature), from mode coupling theory (MCT) [1]. Below $T_c$ supercooled liquids have a non-Debye behavior of relaxation function and non-Arrhenius behavior of the temperature dependence of the relaxation time (or the viscosity) [2–6]. For a recent review, see [7, 8] and references therein. From a variety of experiments [9–12] and simulations [13, 14] it has been shown that at the same point in temperature at which the non-Arrhenius regime is entered from above, glass-forming systems develop heterogeneities in their dynamics, i.e. a distribution of mobilities in the system. In parallel to these experimental activities, different theories for the evolution of glassy dynamics have been developed [15–21], which attribute decoupling of diffusion and viscosity flow to collective effects. Namely, many theories envisage a supercooled liquid as a heterogeneous mixture of clusters, domains, locally favored or frustration-limited structures. But, up to now, many aspects of the characterization of these dynamical heterogeneities have remained elusive. For instance, there is no clear consensus on their shape, size or evolution with temperature.

In our previous works devoted to the vitrification process in the glass-forming substances benzophenone and 2-biphenylmethanol (2BPM) we drew attention to their liquids being possible to cool below their freezing points without crystallizing; however their glassy phases crystallize on heating just after the glassy state becomes a liquid state (cold crystallization) [22–25]. In view of the fact that crystal growth never proceeds without a crystal nucleus, we have concluded that nuclei appear in the supercooled liquid during cooling. Moreover, we have demonstrated experimentally by a differential scanning calorimetry (DSC) technique that generation of the crystal nuclei begins in supercooled liquid benzophenone at 243 K [22] and in 2BPM at 283 K [24], which is about $1.2T_g$. We would draw attention that the crossover temperature $T_c$ is also about $1.2T_g$. Such nuclei appear and disappear in time with dimensions in the range of the critical radius of nucleation before they would be incorporated into the glass structure. Thus, the glassy state we can describe as a mixed phase composed of the crystal nuclei and the interstitial volumes between them. Also it was shown that the nuclei that formed in the supercooled liquid have the crystalline structure of the metastable phase. In both compounds the metastable phase is monoclinic and consists of linear chains of molecules,

[3] Author to whom any correspondence should be addressed.

 

while the structure of the stable phase of benzophenone is orthorhombic [26] and that of 2BPM is triclinic [24]. Their metastable phases have a lower density compared to their stable phases.

The question arises is the nucleation at $T_c = 1.2T_g$ a property of many supercooled systems, or is it a peculiarity of 2BPM and benzophenone? In order to prove this, salol was chosen because of its model glass-forming status, known high fragility, and the wealth of experimental studies of the glass transition with various spectroscopic techniques, such as Brillouin [26, 27] and Raman scattering [28–31], optical Kerr effect spectroscopy [32–34], dielectric spectroscopy [35, 36], photon correlation spectroscopy [37, 38], and longitudinal detected electron spin resonance spectroscopy [39].

This work focuses principally on the determination of the temperature at which the nucleation process starts in the supercooled liquid state of salol, and what kinds of nuclei are generated. For this purpose we have used the DSC method. The obtained data have been compared with that for benzophenone. Also we have studied the Raman spectra upon a different course of temperature change from a liquid to glassy state and back, and their evolution with time at room temperature in order to obtain information on the type of nuclei.

## 2. Experimental methods

The thermal properties were measured with a Perkin-Elmer differential scanning calorimeter equipped with the CCA-7 low-temperature accessory. Samples of salol were introduced in aluminum pans, hermetically scaled using a sample encapsulating press. Liquid nitrogen was used as a coolant and the measurements were carried out in the temperature range 104–333 K.

Raman spectra were measured in a 90° scattering configuration with a double monochromator (Jobin-Yvon Ramanor U 1000 spectrometer), equipped with a standard photomultiplier detector controlled by the Spectra Max software. The dispersion was 9.2 $cm^{-1}$ $mm^{-1}$ at 514.5 nm. The stray light rejection was $10^{-14}$ at 20 $cm^{-1}$ from the Rayleigh line. The spectral slit width was 2 $cm^{-1}$. The spectra were recorded using the 514.5 nm line of an Ar+ laser and the laser beam power focused on a sample was about 150 mW. For measurements at low temperatures salol was confined in thin glass capillaries which were mounted on the copper finger of a Diplex closed-cycle cryostat that can be operated in the temperature range 330–12 K.

## 3. Structure information

Salol [phenyl salicylate, or phenyl-2-hydroxybenzoate; 2-$(OH)C_6H_4CO_2C_6H_5$] of 99% purity was purchased from Aldrich and used without further purification. The chemical structure of salol is shown in the inset of figure 1. The molecule is an asymmetric one consisting of two phenyl rings, which are connected by three single bonds through two, carbon and oxygen, atoms. One hydroxyl group is attached on one of the phenyl rings in the ortho-position.

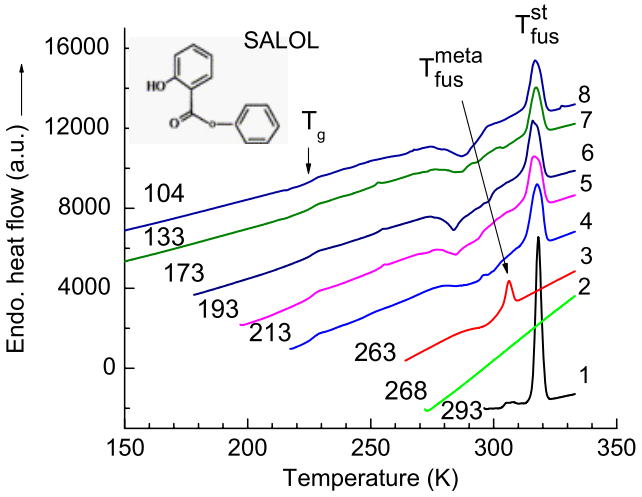


**Figure 1.** DSC heating curves for salol obtained at a heating rate of 20 K $min^{-1}$. Each sample was previously cooled at 200 K $min^{-1}$ from 333 K to the temperature indicated in the figure, and after that immediately reheated. The sample mass is 4.77 mg.

Salol is known to demonstrate two crystalline morphologies, metastable and stable phases, with respective melting points of 302 and 315 K [40]. The stable phase is orthorhombic with space group $P2_12_12_1$ [41] and appears to be extensively investigated. Metastable phase appears as a low-melting crystal having a monoclinic structure with a space group $P2_{1/n}$ [42]. The unit cell of the metastable salol is approximately half that of the stable phase and it contains four molecules as opposed to the eight found in the stable modification. Metastable salol has a lower density ($D_c = 1.350$ g $cm^{-3}$) compared to the stable one ($D_c = 1.357$ g $cm^{-3}$) [42].

It should be noted that spectroscopic information is only available for the stable phase in the literature.

## 4. Results

### *4.1. Thermal behavior*

The thermal behavior of Salol has been studied previously using adiabatic calorimeters [43, 44] and DSC [40, 45]. It was found that this compound can be easily supercooled and vitrified by further cooling. Furthermore, it has been shown that glassy salol crystallizes on heating (cold crystallization). Two different polymorphs were detected. One stable polymorph that melts at $T_{fus} = 315$ K, the other being metastable with $T_{fus} = \sim 301.5$ K. The glass transition temperature $T_g$ was found to be 221 K (onset temperature). For more information see [40, 43–45]. The fact that liquid salol does not crystallize on cooling and its glassy phase crystallizes on heating confirms our assumption that nuclei emerge in the liquid sample during the quenching procedure. Our interest is in the determination of the temperature at which the process of nucleation starts (hereafter $T_n$) in salol. For this purpose we will use the DSC method, which has been applied and described in detail in our previous works [22, 24].

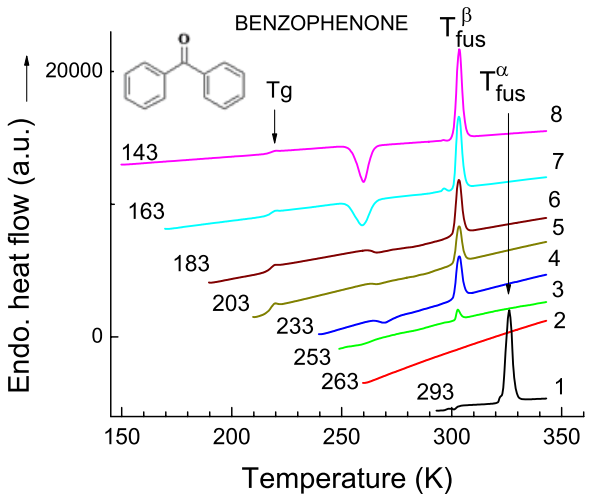


**Figure 2.** DSC heating curves for benzophenone obtained at a heating rate of 20 K min$^{-1}$. Each sample was previously cooled at 200 K min$^{-1}$ from 333 K to the temperature indicated in the figure, and after that immediately reheated. The sample mass is 5.03 mg.

We will compare the thermal behavior of salol with that for benzophenone.

Figures 1 and 2 show DSC heating curves all obtained at a heating rate of 20 K min$^{-1}$ for salol and benzophenone, correspondingly. Each liquid sample for DSC measurement was previously quenched (200 K min$^{-1}$) from 333 K to the temperature (precooling temperature) indicated in the figures 1 and 2, and then measured on heating to examine if crystallization (exothermic peak) and melting (endothermic peak) appear on the DSC curves. Due to the fact that crystallization begins with formation of crystal nuclei, their formation can be judged from the appearance of corresponding peaks on the DSC curve. The sample was kept for 15 min at temperature 333 K, well above the melting temperatures, in order to remove any nuclei that may have formed.

Figure 1 shows eight DSC curves for salol with mass of 4.77 mg. The curves are vertically shifted for the sake of clarity. For the first, the crystalline sample (powder) was heated up from room temperature to 333 K to melt (curve 1). The heating curve 1 shows a relatively sharp single endothermic peak at $T^{st}_{fus} = 318.2$ K, which corresponds to the melting of the stable phase. The crystalline salol starts to melt at the onset temperature 315.8 K. The melting enthalpy was determined to be 88.9 J g$^{-1}$. Curve 2 was obtained for the sample precooled to 268 K. We have not seen any endothermal peak due to melting. The next curve 3 for the liquid sample precooled to 263 shows a tiny melting peak with a very small enthalpy (∼7.6 J g$^{-1}$). The maximum intensity of the melting peak occurred at $T^{meta}_{fus} = 305.8$ K (onset temperature 303.5 K). Consider that the melting peak presupposes the presence of crystal nuclei; we can conclude that the nucleation process in supercooled salol starts at about 263 K. Furthermore the crystalline phase that melts at $T^{meta}_{fus} = 303.5$ K is the metastable phase according to literature data. Thus there exists in the supercooled liquid salol a temperature $T_n$ which separated two liquid states. Above $T_n$ we have to deal with a usual liquid, while below $T_n$ the supercooled liquid is composed of nuclei of the metastable phase. The temperature $T_n = 263$ K is close to the crossover temperature $T_c = 1.2T_g$ (267 K). Therefore, we can conclude that the origin of the crossover at $T_c$ is related to the microscopic structure, namely, to the appearance of fluctuating metastable nuclei in the supercooled liquid.

For the sample precooled below the glass transition temperature in the DSC heating curves three essential features are seen (figure 1, curves 4–8). The first one corresponds to a glass transition at temperature $T^{max}_g = 225.8$ K ($T^{onset}_g = 223$ K), the second is a wide exothermal complex peak that corresponds to cold crystallization and is observed in the temperature interval between 280 and 302 K. It can be seen that the exothermal signal of cold crystallization is strongly sensitive in shape to changes in the precooling temperature. The third large endothermic melting peak, at $T^{st}_{fus} = 318.2$ K, indicates melting of the stable polymorph. Taking into account that the metastable modification of salol is able to undergo a solid–solid monotropic transformation into the stable form [42], we can conclude that the wide exothermal complex peaks which is seen in the curves 4–8 (figure 1) in the temperature interval 280–302 K correspond to the interconversion of the metastable phase into the stable one. This would explain why melting of the metastable phase is not seen. Such interconversion between two polymorphs of salol was also demonstrated in [40].

Figure 2 shows DSC heating curves for benzophenone at seven precooling temperatures for a sample with mass of 5.03 mg. The curves are vertically shifted. As in the case of salol we firstly melt the crystalline sample (powder) to obtain the liquid phase (curve 1). The heating curve 1 shows a relatively sharp single endothermic peak at $T^{\alpha}_{fus} = 326.2$ K (onset 325.5), which corresponds to the melting of the stable phase ($\alpha$-phase). Curve 2 was obtained for the liquid sample precooled to 263 K. We have not seen any endothermal peak due to melting. The next curve 3 for the liquid sample precooled to 253 K shows a melting peak with an enthalpy of 5.9 J g$^{-1}$. The maximum intensity of the melting peak occurred at $T^{\beta}_{fus} = 302.6$ K (onset temperature 301.2 K). The observed melting peak corresponds to the melting temperature of the metastable phase of benzophenone ($\beta$-phase). The next curve 4 for the liquid sample precooled to 233 K, shows a small single exothermal peak at 260 K that corresponds to the crystallization, and a small melting peak at $T^{\beta}_{fus} = 303.2$ K (onset 300.8 K) with an enthalpy of ∼10 J g$^{-1}$. In the cases of precooling temperatures 203, 183, 163 and 143 K, which are below the glass transition temperature $T_g = 211.7$ K (figure 2, curves 5–8) the enthalpy of melting increases from 10 J g$^{-1}$, reaching values of 20.6, 39.2 and 80.0 J g$^{-1}$, respectively.

The analysis of the DSC curves allows us to conclude that the nucleation process starts at $T_n = 253$ K and proceeds to the glassy state. The average fraction of the metastable phase (enthalpy) increases with decreasing temperature and tends to saturate at temperatures below $T_g$. It is seen that the experimentally found $T_n = 253$ K, at which nucleation starts in supercooled liquid benzophenone, is in reasonably good agreement with the crossover temperature $T_c = 1.2T_g$ (254 K).

It is necessary to emphasize that the temperature behavior shown in figure 2 is not always strictly observed. Often the

monotropic transition from the metastable benzophenone to stable phase occurs as in the case of salol. An example of such a transition is presented in figure 1 of [22], where it has been found that the process of nucleation in benzophenone starts at 243 K. The difference in the temperatures where nucleation starts in different DSC experiments is due to the fact that nucleation and crystal growth are somewhat probabilistic events with the consequence that the experiments are not entirely reproducible.

Another interesting finding is that in the case of a very small sample mass (<1 mg) of salol, benzophenone, or 2BPM the crystallization does not occur in their supercooled liquids. This finding is consistent with the crystallization behavior of liquids in porous glasses [46, 47].

Our results testify that the glassy state is composed of the crystalline nuclei. The question that remains is whether the crystalline structure of the metastable phase coincides with the structure of the stable phase or not? This question arises in connection with the papers devoted to the low-temperature crystallization in the glass transition region of salol [43, 44], benzophenone [43], o-terphenyl [48], and triphenylethylene [49]. There have been reports about two types of the crystallization rates in the different temperature ranges. However, the authors of [43, 44] on the basis of the powder x-ray diffractometry experiments have stated that metastable crystals of salol and benzophenone formed at low temperatures and their stable crystals formed at high temperatures have the same crystal structure. Some doubts are cast upon the validity of this statement because benzophenone [50] and salol [41, 42] are known to have a monotropic transition from the metastable phase to the stable one, thus an x-ray study of the metastable phase would meet with difficulties.

To be sure that the crystalline structure of the metastable phase of salol differs from that of the stable phase we have performed a low-frequency Raman spectroscopy investigation.

### *4.2. Low-frequency Raman spectra*

Low-frequency Raman measurements were as follows: (1) a powder of crystalline salol was melted in a glass capillary tube by heating to 370 K; (2) the liquid sample was then cooled down to 70 K and during cooling the low-frequency Raman spectra were recorded (figure 3); (3) the glassy salol is then heated up to room temperature and low-frequency spectra were recorded on heating (figure 5).

The inset in figure 3 shows three Raman spectra of the liquid sample at temperatures 293, 270 and 250 K. It is well known that the Raman spectra of liquids are dominated by a quasielastic relaxational contribution that is quasielastic scattering (QS, the strong scattering line spreading out about zero frequency). As can be seen in the inset, the QS component decreases strongly with decreasing temperature. Upon cooling through the glass transition temperature ($T_g$ = 224 K) and lowering down to 70 K, the decrease of the QS component leads to the observation of a broad low-frequency band in the spectral range 14.5–17.2 cm$^{-1}$. This band has been named the boson peak (BP), a universal property of all

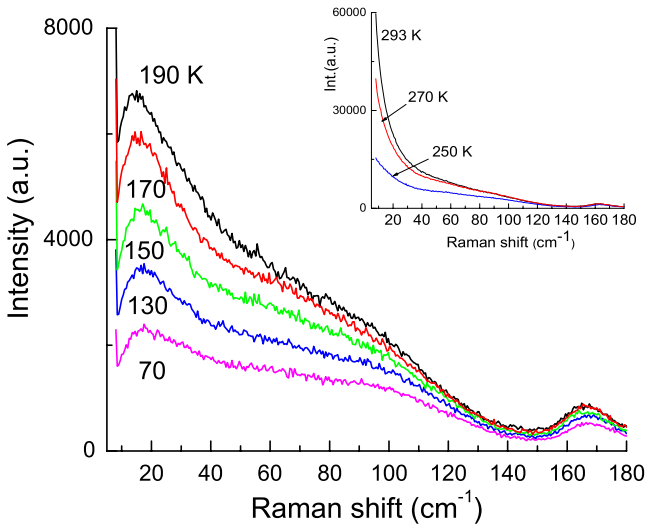


**Figure 3.** Evolution of the low-frequency Raman spectra of salol with decreasing temperature from 190 to 70 K. The initial state is liquid salol. Temperature is given in K. Inset: low-frequency Raman spectra at 293, 270, and 250 K.

glasses. A number of models have been developed in order to explain the boson peak [51–62], and the list of references given here is by no means complete. In particular, the BP was attributed to structural defects [51], localized excitations in the framework of the soft-potential model [52], or to cooperative vibrational modes localized resonantly to locally favored structures [56, 57]. Recently, a possibility that the origin of the boson peak is due to transverse vibrational modes associated with defective soft structures in the disordered state was proposed in [58]. In some models it is assumed that the existence of the medium range order and cohesion inhomogeneities in disordered media is responsible for the BP. The medium range order implies that the arrangement of structural units in a glass is not completely random but has some correlations on a nanometer scale (a nano-scale inhomogeneity) [59–62]. Despite intensive studies by both experimentalists and theorists over the last three decades, the origin of the BP is still far from being completely understood.

The spectral form of the first-order vibrational part has been described by the following relation [54] $I_{\rm exp}(\omega) = C(\omega)g(\omega)[n(\omega,T)+1]\omega^{-1}$, where $C(\omega)$ is the photon–phonon coupling coefficient, $n(\omega,T) = [\exp(h\omega/\kappa_{\rm B}T) - 1]^{-1}$ is the Bose–Einstein occupation number, $g(\omega)$ is the vibrational density of states. Usually depolarized light scattering $I_{\rm exp}(\omega)$ is converted into reduced spectral density $I_{\rm red}(\omega) = I_{\rm exp}(\omega)/[n(\omega,T)+1]\omega \sim C(\omega)g(\omega)/\omega^2$. In practice, $I_{\rm red}(\omega) \approx T^{-1}I_{\rm exp}(\omega)$ since $[n(\omega,T)+1]^{-1} \sim h\omega/\kappa_{\rm B}T$ for $h\omega/\kappa_{\rm B}T \ll 1$. Another frequently used spectral reduction approach is the conversion into Raman susceptibility $\chi'' = I_{\rm exp}(\omega)/[n(\omega,T)+1] \sim C(\omega)g(\omega)/\omega$. $C(\omega)$ usually has a linear frequency dependence in the spectral region of the boson peak [61]. Consequently, the Raman susceptibility can be considered to be representative of the vibrational density of states ($g(\omega)$, VDOS) in the low-frequency range.

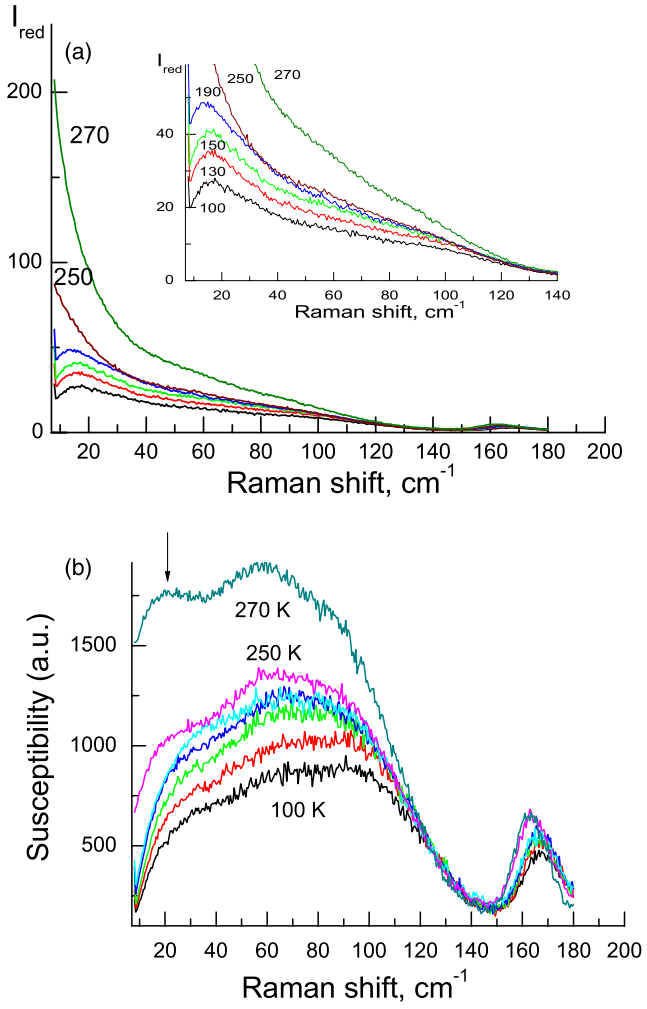


**Figure 4.** (a) Temperature-dependent Raman spectra of salol normalized by the temperature factor $[n(\omega, T) + 1]$. The temperatures are (top to bottom): 270, 250, 190, 150, 130, and 100 K. Inset: the same as in the main figure but expanding the intensity axis. (b) Temperature-dependent Raman susceptibilities of salol. The temperatures are (top to bottom): 270, 250, 190, 170, 150, 130, and 100 K. The arrow denotes the frequency of the BP.

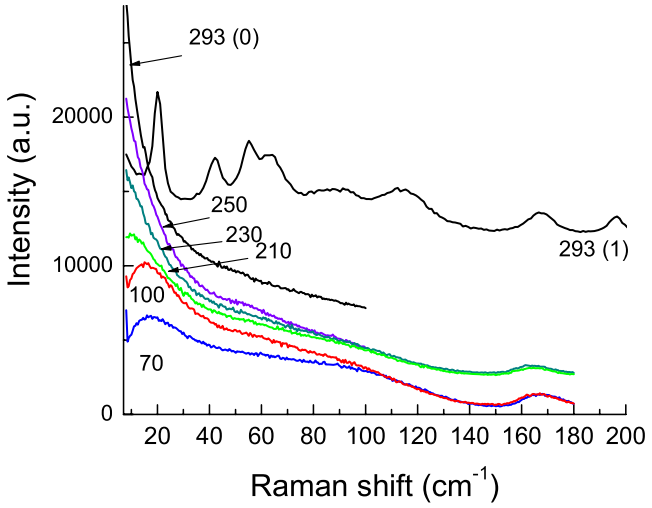


**Figure 5.** Evolution of the low-frequency Raman spectra of salol with increasing temperature from 70 K to room temperature (see the text for details). The initial state is glassy salol. Temperature is given in K.

Figure 4, parts (a) and (b), show the reduced representation of the low-frequency Raman spectra $I_{\rm red}(\omega)$ (figure 4(a)) and the low-frequency Raman susceptibilities $\chi''$ (figure 4(b)) recorded at different temperatures. Figure 4(a) shows a decrease of the quasielastic component. The decrease of the low-frequency intensity leads to the observation of a BP with a maximum intensity around 15 $\rm cm^{-1}$. The low-frequency Raman susceptibility of the supercooled liquid (270 and 250 K) is characterized by two broad vibrational bands with a maximum near 20 and 65 $\rm cm^{-1}$ below 140 $\rm cm^{-1}$ and the band at 169.6 $\rm cm^{-1}$ which corresponds to the intramolecular vibration (figure 4(b)). The arrow indicates the region where in the reduced Raman spectra the BP is present. In the temperature range <190 K the Raman susceptibility of the glassy state gradually changes with decreasing temperature. The band at 20 $\rm cm^{-1}$ in the liquid state becomes a shoulder in the glassy state (figure 4(b)).

Figure 5 shows Raman spectra recorded upon heating from 70 K through the glass transition where the glassy phase becomes a liquid phase. It is seen that with increasing temperature the BP is obscured by the increase of the QS intensity. This is an indication on the appearance of liquid during transformation of the glassy phase into liquid above $T_{\rm g}$. The curve denoted 293(0) shows the spectrum which was recorded immediately after approaching room temperature, the next curve 293(1) was recorded 30 min after recording the curve marked 293(0). Remarkable changes become evident: the QS line disappears and new sharp bands appear, corresponding to the lattice vibrations, as expected for a crystalline phase. Once transformed, no further evolution of the spectrum was observed. This means that within 30 min the crystallization process was completed.

In figure 6, we compare the Raman spectrum of the stable crystalline phase (curve 1) with this newly emerging (metastable) phase (curve 2). It is clear that if the crystalline structures of these two phases are different then the lattice vibration frequencies should also be different. In accordance with expectation it is seen that the lattice vibration frequencies in the Raman spectra of the metastable phase are clearly distinguished from those in the stable one. The spectrum of the stable phase begins from the lowest lattice vibration centered at 17.1 $\rm cm^{-1}$, while the spectrum of the metastable phase begins from 20.4 $\rm cm^{-1}$. All other frequencies of the lattice bands in these phases also fail to coincide. In the metastable phase lattice vibrations are situated at 20.4, 42.5, 55.3, 63.0, 89.0, 112.6 $\rm cm^{-1}$, while in the stable phase they are situated at 17.1, 30.3, 36.5, 40.5, 62.0, 66.5, 78.7, 100.0 $\rm cm^{-1}$. The frequencies of the last three bands at 167.3, 196, 248.3 $\rm cm^{-1}$ in these spectra almost coincide. According to [63] they are related to the intramolecular vibrations: out-of-plane deformational vibrations (167.3, 248.3 $\rm cm^{-1}$) and in-plane stretching vibrations (196.0 $\rm cm^{-1}$) of the phenyl rings.

Another fact which confirms the formation of the metastable phase is that the metastable phase transforms into a liquid in the capillary which was taken out of the holder and

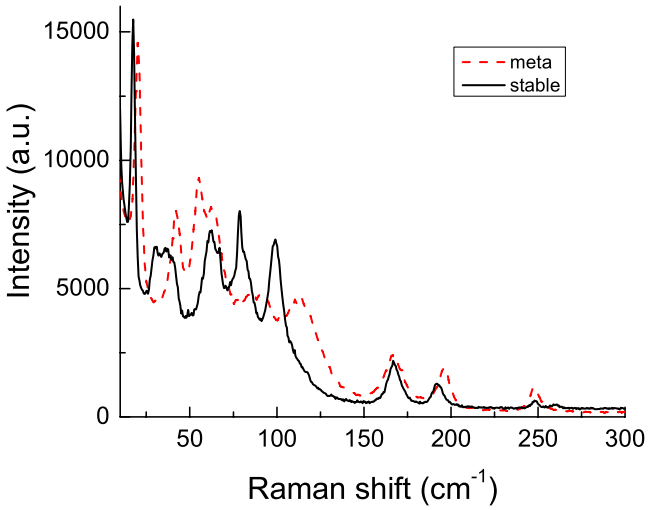


**Figure 6.** Low-frequency Raman spectra of the stable (solid curve) and metastable (dashed curve) phases of salol at room temperature.

kept in the hand. Such transformation can occur only with the metastable phase that melts at 30.5 °C.

The reduced Raman spectrum $I_{\mathrm{red}}(\omega)$ (figure 7(a)) and the Raman susceptibility $\chi''(\omega)$ (figure 4(b)) of the metastable crystal were recorded at 170 K to be compared to the $I_{\mathrm{red}}(\omega)$ and $\chi''(\omega)$ spectra of the glassy state at the same temperature. It is clearly revealed by figure 7(a) that the phonon peak frequency in the metastable phase at 22.3 cm$^{-1}$ and the position of the BP at 14.8 cm$^{-1}$ in the reduced Raman spectra do not coincide. By this it is possible to conclude that the BP is not the result of a broadening of the phonon peak. However, in the Raman susceptibility spectra (figure 7(b)), the phonon band at 22.3 cm$^{-1}$ in the crystal exhibits a correspondence with the low-frequency shoulder of the wide band in the glassy state. Also the frequencies of the most intense phonon bands at 58.8 and 68.8 cm$^{-1}$ are very close to the maximum of the wide band at 65 cm$^{-1}$ in the glassy state.

It is evident that the spectrum of Raman susceptibility of the glassy salol reflects the existence of underlying broad phonon peaks. We consider this fact as a confirmation of the presence of nuclei in the glassy state (medium range order). The broadening of phonons could be due to a confinement effect in the nanonuclei.

## 5. Discussion

It should be noted that in the most popular MCT model [1] which is used to interpret many experiments, the mechanism responsible for the slow dynamics has been considered to be completely independent of the nucleation process. In contrast to the MCT model our experimental results testify that below a crossover temperature $T_{\mathrm{c}}$, where a complicated relaxation process was observed in many glass formers (including salol, benzophenone and 2BPM), the metastable nuclei are generated. Thus the MCT model could not be used for describing the experimental results, at least for these compounds. On the other hand, we can conclude that the slow

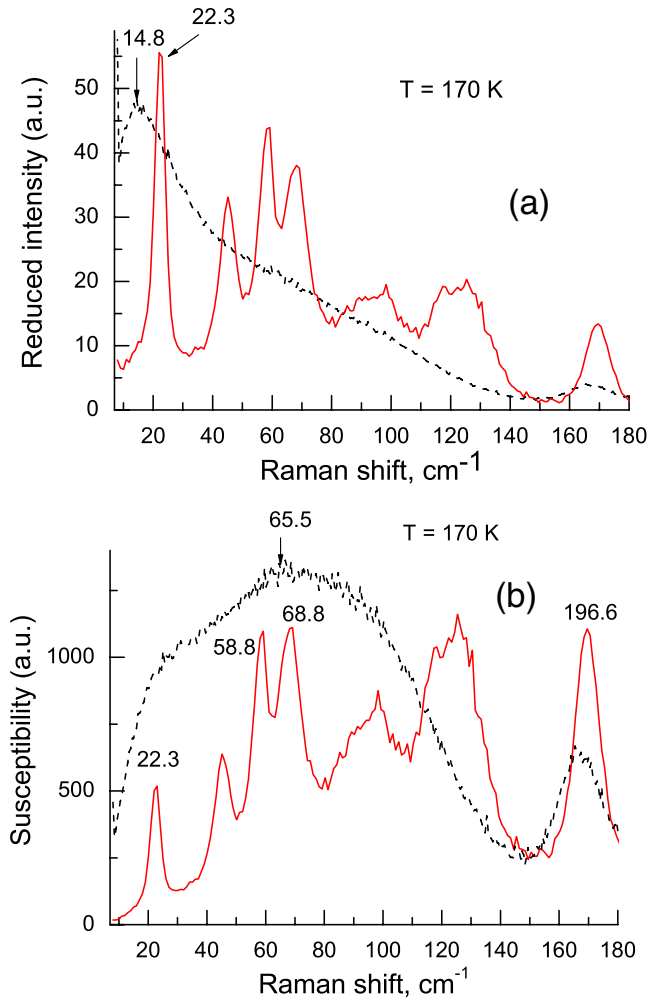


**Figure 7.** (a) Low-frequency reduced Raman spectra of the metastable (solid curve) and glassy (dashed curve) phases of salol at 170 K. (b) Low-frequency Raman susceptibilities of the metastable (solid curve) and glassy (dashed curve) phases of salol at 170 K.

relaxation of the nuclei should give rise to the slow relaxation of the supercooled liquid below $T_{\mathrm{n}}$ ($T_{\mathrm{c}}$), and the finite lifetime of nuclei should give rise to dynamic heterogeneity of the supercooled liquid. The increase (decrease) in the nuclei size may be responsible for the fast relaxation ($\beta$-process).

In this context it is interesting to pay attention to the experimental works in which the process of nucleation in supercooled liquids was also observed. Low-temperature crystal growth was investigated in many other fragile liquids, such as salol [43, 44], benzophenone [43], o-terphenyl [64, 65], triphenylethylene [43], toluene [66], iso-propylbenzene [67], dimethylphthalate [67], and diphenylphthalate [67] using an optical microscope. The authors of [67], based on experimental results, claimed 'that the embryos are formed in any supercooled liquid at low temperatures'.

Recently, Kurita and Tanaka [68] observed the nucleation-growth-type liquid–liquid transition in n-butanol. The authors of [68] described that macroscopic droplets of nucleated liquid II contains microcrystallites, which exhibit optical birefringence. (For more details see [68].) More recently, Hassaine *et al* [69] reported the investigation of n-butanol in

the wide low-temperature range using different techniques. Their experimental results show that the obtained 'glacial' state (first reported to occur in triphenyl phosphite (TPP) [70]) is not a homogeneous amorphous state but rather a mixture of two different coexisting phases, very likely the (frustrated) crystal phase embedded in a disordered glassy phase. Hedoux *et al* [71] in their study of n-butanol reported that the devitrification of n-butanol can be described by a classical nucleation growth law. It should be noted that the nature of the 'glacial' state remains controversial. The heterogeneous description for this state in TPP is proposed by Hedoux *et al*, whereby the 'glacial' state would be a biphased phase constituted by a mixture of nano- to microcrystallites—depending on $T_a$, amorphous-like for 210 K $< T_a <$ 216 K and crystal-like for 216 K $< T_a <$ 230 K—of the hexagonal crystal phase embedded within the untransformed supercooled liquid, forming a heavily nucleated state [72–74]. Tanaka *et al* also considered two regimes within the temperature range where the 'glacial' state is formed [75, 76]. Below a spinodal-decomposition temperature ($T_{sd} \sim$ 216 K), a homogeneous phase is observed: the 'glacial' state would be the glassy state of a second liquid II (glass II). Above $T_{sd}$, the observed phase is heterogeneous, and the 'glacial' state would be a mixture of glass II and microcrystallites of the crystal phase. According to Oguni *et al* [77] the 'glacial' state is a highly correlated second liquid.

Our experimental findings point toward the major role of nucleation in the vitrification of supercooled liquids. It should be emphasized that if the nuclei of the stable phase remain in the liquid phase after its melting, we could not avoid crystallization during cooling of this melt. To avoid crystallization the liquid sample should be kept well above the melting temperature for 15 min or more in order to remove any nuclei that may have formed. In that case a sample of liquid salol will not crystallize for years in a glass capillary at a room temperature. More importantly, even if we avoid crystallization of the stable phase during cooling, we cannot avoid the nucleation of the metastable nuclei below $T_n$ temperature. They appear regardless of the rate of cooling (fast quenching or slow cooling). On lowering the temperature of the supercooled liquid below $T_g$ the glass phase preserves these nuclei. After melting of the glassy salol the size of nuclei increases and cold crystallization occurs. However, the rate of metastable crystal growth is very low in comparison with that for the stable one. We are reminded that the metastable phase is monoclinic and consists of hydrogen-bonded chains of molecules. It looks like such an arrangement of the molecules retards the growth of nuclei. The retarded crystallization of the metastable phase also has been observed for benzophenone and 2BPM. Their metastable structures also consist of molecules which are arranged in chains.

The first attempt to explain a glass transition, focusing directly on density ordering (or crystallization) has been made in a two-order parameter model of the liquid–glass transition proposed by Tanaka [19–21, 56–58, 78–80]. This model is based on the physical picture that there exist locally favored structures in any liquids, which are temporally formed by the active local bonds between molecules to minimize the local bonding energy. They have a symmetry that is frustrated and inconsistent with a crystallographic symmetry of the equilibrium crystal and causes frustration against crystallization. This theory primarily ascribes glassy dynamics to the growth of medium range crystal-like bond orientational order under the frustration effects of locally favored structures (which act as impurities for crystallization). Thus, it is natural to make a connection between this medium range crystal-like order to metastable nuclei, which are formed in supercooled liquid salol on cooling.

## 6. Conclusion

We have studied the supercooled and crystalline phases of salol by DSC and Raman scattering experiments. Each method clearly provides evidence that in the supercooled liquid fluctuating metastable nuclei are formed below $T_n$, which is close to $T_c = 1.2T_g$. The crystalline structure of these metastable nuclei is not consistent with that of the initial crystal. It is monoclinic, and composed of molecules grouped in chains, which are stabilized by the hydrogen bonding interaction. The melting temperature and density of the metastable phase are lower than that of the stable phase. Below $T_g$ these nuclei turn out to be incorporated in the glass structure and considered as a measure of the intermediate range order in this glass. The BP peak in the low-frequency Raman spectrum of the glassy phase reflects the presence of these nuclei with typical sizes in the nanometer range.

Experimental results presented in this paper are evidence for the crucial role of nucleation in the vitrification of supercooled liquid salol as well as benzophenone and 2BPM. We believe these results should stimulate further work on other glass formers before any generalization is concluded.

## Acknowledgment

The detailed constructive comments of two anonymous referees are appreciated.

## References

[1] Gotze W and Sjogren L 1992 *Rep. Prog. Phys.* **55** 241
[2] Andreozzi L, Faetti M and Giordano M 2006 *J. Non-Cryst. Solids* **352** 3829
[3] Sillescu H 1999 *J. Non-Cryst. Solids* **243** 81
[4] Debenedetti P G and Stillinger F H 2001 *Nature* **410** 259
[5] Angell C A, Ngai K L, McKenna G B, McMillan P F and Martin S W 2000 *J. Appl. Phys.* **88** 3113
[6] Ediger M D, Angel C A and Nagel S R 1996 *J. Phys. Chem.* **100** 13200
[7] Angel C 2008 *J. Non-Cryst. Solids* **354** 4703
[8] Hecksher T, Nielsen A I, Olsen N B and Dyre J C 2008 *Nat. Phys.* **4** 737
[9] Cicerone M T and Ediger M D 1995 *J. Chem. Phys.* **103** 5684
[10] Schiener B, Bohmer R, Loidl A and Chamberlin R V 1996 *Science* **274** 752
[11] Richert R 1997 *J. Phys. Chem.* B **101** 6323
[12] Eckstein E, Qian J, Hentschke R, Thurm-Albecht T, Steffen W and Fischer E W 2000 *J. Chem. Phys.* **113** 4731
[13] Donati C, Douglas J F, Kob W, Plimpton S J, Poole P H and Glotzer S C 1998 *Phys. Rev. Lett.* **80** 2338

[14] Buchner S and Heuer A 2000 *Phys. Rev. Lett.* **84** 2168
[15] Cohen I, Ha A, Zhao Z, Lee M, Fischer T, Strouse M J and Kivelson D 1996 *J. Phys. Chem.* **100** 8518
[16] Kivelson D, Kivelson S A, Zhao X L, Nussinov Z and Tarju G 1995 *Physica* A **219** 27
[17] Adam G and Gibs I H 1965 *J. Chem. Phys.* **43** 139
[18] Cohen M H and Grest G S 1979 *Phys. Rev.* B **20** 1077
[19] Tanaka H 2005 *J. Non-Cryst. Solids* **351** 3385
[20] Kurita R and Tanaka H 2005 *J. Phys.: Condens. Matter* **17** L293
[21] Sintani H and Tanaka H 2006 *Nat. Phys.* **2** 200
[22] Davydova N A, Mel'nik V I, Baran J and Drozd M 2003 *J. Mol. Struct.* **651–653** 171
[23] Davydova N A, Mel'nik V I, Nelipovitch K, Baran J and Kukielski J I 2002 *Phys. Rev.* B **65** 094201
[24] Baran J, Davydova N A, Drozd M and Pietraszko A 2006 *J. Phys.: Condens. Matter* **18** 5695
[25] Baran J, Davydova N A and Drozd M 2007 *J. Non-Cryst. Solids* **353** 1793
[26] Du W M, Li G, Cummins H Z, Fuchs M, Toulouse J and Knauss L A 1994 *Phys. Rev.* E **49** 2192
[27] Dreyfus C, Lebon M J, Cummins H Z, Toulouse J, Bonello B and Pick R M 1992 *Phys. Rev. Lett.* **69** 3666
[28] Pratesi G, Bellosi A and Barocchi F 2000 *Eur. Phys. J.* B **18** 283
[29] Li G, Du W M, Sakai A and Cummins H Z 1992 *Phys. Rev.* A **46** 3343
[30] Cummins H Z, Du W M, Fuchs M, Gotze W, Hildebrand S, Latz A, Li G and Tao N J 1993 *Phys. Rev.* E **47** 4223
[31] Kalampounias A G, Kirillov S A, Steffan W and Yannopoulos S A 2003 *J. Mol. Struct.* **651–653** 475
[32] Hinze G, Brace D D, Gotke S D and Fayer M D 2000 *Phys. Rev. Lett.* **84** 2437
[33] Cang H, Novikov V N and Fayer M D 2003 *J. Chem. Phys.* **118** 2800
[34] Cang H, Novikov V N and Fayer M D 2003 *Phys. Rev. Lett.* **90** 197401
[35] Casalini R, Paluch M and Roland C M 2003 *J. Phys. Chem.* A **107** 2369
[36] Stickel F, Fischer E W and Richert R 1995 *J. Chem. Phys.* **102** 6251
[37] Brodin A, Bergman R, Mattsson J and Rossler E A 2003 *Eur. Phys. J.* B **36** 349
[38] Comez L, Corezzi S, Fioretto D, Kriegs H, Best A and Steffen W 2004 *Phys. Rev.* E **70** 011504
[39] Andreozzi L, Faetti M and Giordano M 2006 *J. Non-Cryst. Solids* **352** 3829
[40] Ramos J M, Correia N T and Dioglo H P 2004 *Phys. Chem. Chem. Phys.* **6** 793
[41] Bilgram J H, During U, Wachter M and Seiler P 1982 *J. Cryst. Growth* **57** 1
[42] Hammond R B, Jones M J, Roberts K J, Kutzke H and Klapper H 2004 *Z. Kristallogr.* **217** 484
[43] Hanaya M, Hikima T, Hatase M and Oguni M 2002 *J. Chem. Thermodyn.* **34** 1173
[44] Hikima T, Hanaya M and Oguni M 1995 *Solid State Commun.* **93** 713
[45] Paladi F and Oguni M 2003 *J. Phys.: Condens. Matter* **15** 3909
[46] Rengarajan G T, Enke D and Beiner M 2007 *Open Phys. Chem. J.* **1** 18
[47] Jackson C L and McKenna G B 1990 *J. Chem. Phys.* **93** 9002
[48] Hikima T, Adachi Y, Hanaya M and Oguni M 1995 *Phys. Rev.* B **52** 3900
[49] Hikima T, Hanaya M and Oguni M 1999 *J. Mol. Struct.* **479** 245
[50] Kutzke H, Klapper H, Hammond R B and Roberts K J 2000 *Acta Crystallogr.* B **56** 486
[51] Elliot S R 1992 *Europhys. Lett.* **19** 201
[52] Buchenau U, Galperin Y M, Gurevich V I, Parshin D A, Ramos M A and Schober H R 1992 *Phys. Rev.* B **46** 2798
[53] Gurevitch V L, Parshin D A, Pelos J and Schober H R 1993 *Phys. Rev.* B **48** 16318
[54] Shuker R and Gammon R W 1970 *Phys. Rev. Lett.* **25** 122
[55] Martin J and Brenig R W 1974 *Phys. Status Solidi* b **64** 163
[56] Mermet A, Surovtsev N V, Duval E, Jal J, Dupuy-Philos J and Dianous A 1996 *Europhys. Lett.* **36** 277
[57] Malinovsky V K and Sokolov A P 1986 *Solid State Commun.* **57** 757
[58] Malinovsky V K, Novikov V N, Parshin P P, Sokolov A P and Zemlyanov M G 1990 *Europhys. Lett.* **11** 43
[59] Schroeder J, Wu W, Apkarian J L, Lee M, Hwa L-G and Moynihan C T 2004 *J. Non-Cryst. Solids* **349** 88
[60] Duval E, Etienne S, Simeoni G and Mermet A 2006 *J. Non-Cryst. Solids* **352** 4525
[61] Duval E, Boukenter A and Achibat T 1990 *J. Phys.: Condens. Matter* **2** 10227
[62] Appignanesi G A and Fris J A R 2009 *J. Phys.: Condens. Matter* **21** 203103
[63] Hanuza J, Sasiadek W, Michalski J, Lorenc J, Marczka M, Kaminslii A A, Butashin A V, Klapper H, Hulliger J and Mohmed Abudelrhman F A 2004 *Vib. Spectrosc.* **34** 253
[64] Hikima T, Adachi Y, Hanaya M and Oguni M 1995 *Phys. Rev.* B **52** 3900
[65] Hikima T, Hanaya M and Oguni M 1998 *J. Non-Cryst. Solids* **235–237** 539
[66] Hatase T, Hanaya M, Hikima T and Oguni M 2002 *J. Non-Cryst. Solids* **307–310** 257
[67] Hatase T, Hanaya M and Oguni M 2004 *J. Non-Cryst. Solids* **333** 129
[68] Kurita R and Tanaka H 2005 *J. Phys.: Condens. Matter* **17** L293
[69] Hassaine M, Jimenez-Rioboo R J, Sharapova I V, Korolyuk O A, Krivchikov A I and Ramos M A 2009 *J. Chem. Phys.* **131** 174508
[70] Ha A, Cohen I, Zhao X, Lee M and Kivelson D 1996 *J. Phys. Chem.* **100** 1
[71] Wypych A, Guinet Y and Hedoux A 2007 *Phys. Rev.* B **76** 144202
[72] Hedoux A, Guinet Y, Derollez P, Hernandez O, Pacon L and Descamps M 2006 *J. Non-Cryst. Solids* **325** 4994
[73] Hedoux A, Guinet Y, Derollez P, Hernandez O, Lefort R and Descamps M 2004 *Phys. Chem. Chem. Phys.* **6** 3192
[74] Derollez P, Hedoux A, Guinet Y, Lefebvre J, Descamps M and Hernandez O 2006 *Z. Kristallogr.* **23** (Suppl.) 557
[75] Tanaka H, Kurita R and Mataki H 2005 *Phys. Rev. Lett.* **92** 025701
[76] Tanaka H 2000 *Phys. Rev.* E **62** 6968
[77] Mizukami M, Kobashi K, Hanaya M and Oguni M 1999 *J. Phys. Chem.* B **103** 4078
[78] Tanaka H 1999 *J. Chem. Phys.* **111** 3175
[79] Tanaka H 2003 *Phys. Rev. Lett.* **90** 055701
[80] Kurita R and Tanaka H 2004 *Science* **306** 845